ISSN 0965-545X, Polymer Science, Ser. A, 2014, Vol. 56, No. 6, pp. 798–811. © Pleiades Publishing, Ltd., 2014.
Original Russian Text © E.A. Karpukhina, S.O. Il'in, V.V. Makarova, I.B. Meshkov, V.G. Kulichikhin, 2014, published in Vysokomolekulyarnye Soedineniya. Ser. A, 2014, Vol. 56, No. 6, pp. 670–684.

Phase State and Rheology of Polyisobutylene Mixtures with Decyl Surface Modified Silica Nanoparticles

E. A. Karpukhina[a], S. O. Il'in[a]*, V. V. Makarova[a], I. B. Meshkov[b], and V. G. Kulichikhin[a]

[a] *Topchiev Institute of Petrochemical Synthesis, Russian Academy of Sciences, Leninskii pr. 29, Moscow, 119991 Russia*
[b] *Enikolopov Institute of Synthetic Polymer Materials, Russian Academy of Sciences, Profsoyuznaya ul. 70, Moscow, 117393 Russia*
**e-mail: s.o.ilyin@gmail.com*

Received April 16, 2014;
Revised Manuscript Received June 9, 2014

Abstract—The miscibility of linear polyisobutylene and silica nanoparticles with surfaces modified by decyl groups is studied. The phase state of these systems corresponds to the amorphous equilibrium and may be described by a binodal with the UCST. As the radius of the inorganic core of nanoparticles and the molecular mass of polyisobutylene increase, the insolubility region on the phase diagram becomes wider. The addition of nanoparticles to the polymer leads to decreases in the viscoelastic characteristics of homogeneous media and provides the non-Newtonian behavior of the composition in the two-phase region. Shear deformation causes shifts of the phase equilibrium lines in the direction depended on the sizes of the nanoparticles.

DOI: 10.1134/S0965545X14060066

INTRODUCTION

Since the appearance of nanocomposites based on polymers, Nicolai Alfredovich Platé demonstrated sincere interest in this area. While observing the process of ordering of clay particles in a solution of polyisobutylene during flow, he said the key phrase "Well, this is the chaos–order transition!" This was the title of a paper that was published in 2009 and served as a basis for a series of studies awarded with the Grand Prize of the Nauka Publishing House. It was Platé who emphasized the relationship between the physical chemistry of polymers and colloidal chemistry in the analysis of such objects. The study of rheological and relaxation properties of macromolecular particles (dendrimers, MQ resins, silicasols) during the advancement of this direction at the Topchiev Institute of Petrochemical Synthesis (jointly with the Enikolopov Institute of Synthetic Polymer Materials) revealed that their behavior is similar to that of colloid systems. It is natural that, at the next stage, mixtures of macromolecular particles with linear macromolecules were analyzed, because the organic shells of silicasols provided their compatibility with conventional polymers, while silica cores is essentially a nanosized filler. This analysis was performed with the use of two main methods: microinterferometry, which makes it possible to estimate the miscibility of components at the optical level, and rheology, which provides a way to ascertain difference in viscoelastic properties in various regions of the phase diagram.

The synthesis and characterization of composite materials is an urgent line of modern science. These systems consist of two to several phases with different compositions and structures. Mixtures make it possible to unite the properties of individual components to some extent and to attain synergistic behavior. Polymer nanocomposites—polymer matrixes containing solid nanoparticles distributed in them—belong to a new class of composite materials. Owing to high dispersion of nanosized filler particles, these systems can feature unusual properties that cannot be achieved by conventional composites [1, 2]. This phenomenon is above all related to the high surface energy of nanoparticles and, as a consequence, to the high adsorption ability with respect to macromolecules of the polymer matrix that are close in polarity to nanoparticles. Therefore, macromolecules in the adsorption layers acquire unnatural, frequently extended conformations; as a result, reinforcement of the polymer occurs even at filler concentrations below the percolation threshold. Components with similar polarities preserve a certain similarity of the chemical structures of interfaces between particles and the adsorption layer of macromolecules of the matrix polymer.

Metals, metal oxides, polymers, semiconductors, aluminosilicates, carbon nanotubes and nanofibers, nanodiamonds, aerosils, and other inorganic and organic compounds are used as fillers for polymer nanocomposites [3–8]. At present, a lot of diverse kinds of polymer nanocomposites have been prepared. Many of them feature valuable properties: enhanced thermal stability and heat resistance, high strength-to-weight ratios, low specific gravities, high water and weather resistance, and chemical inertness [7–11]. Such materials have found use in various industries: They are used to manufacture special coatings, fire-resistant materials, proton-conducting membranes, car components, and microelectronic and micro-optical devices [11–13].

As was mentioned above, the key issue in the design of nanocomposites is to provide a certain level of interaction between particles (or droplets) of the dispersed phase with the polymer dispersion medium. In the case of solid nanometer particles (layered silicates, nanodiamonds, aerosils, etc.), this interaction is implemented only owing to a high adsorption activity of the filler with respect to the polymer, as is typical for nonpolar surfaces with respect to nonpolar polymers and vice versa. If the adsorption interaction is practically absent, as in the case of polar fillers in nonpolar polymers, then inner stresses appear on the interfacial boundaries [14] and, in the limit, the system segregates into two macrophases [15]. Thus, in general, modification of the surfaces of particles seems reasonable for ensuring the desired level of affinity between the particles and the polymer matrix.

Various types of modification of particles promote an increase in their compatibility or even miscibility with a linear polymer matrix and impart the desired properties to it without any change in the nature of the particles [16]. This problem was traditionally solved with the use of surfactant additives. However, in this case, the incorporation of low-molecular-mass compounds or oligomers into the polymer composite worsens the complex of performance characteristics of the composite material [17].

The chemical modification of the filler surface turns out to be more fruitful. There are many examples of this kind; however, each kind of filler requires the use of certain chemical reagents and sometimes the use of their preparation procedures [18, 19]. Silica is the most commonly used filler for polymer compositions. There are several studies devoted to the synthesis of silica particles with modified surfaces. However, almost all of these studies deal with treatment of the surfaces of preformed particles prepared through various methods; that is, in all cases, the problem related to the aggregation of particles during their growth prior to the chemical treatment of the surfaces arises [14, 20].

A new approach to creating silica nanoparticles with modified surfaces (molecular silicasols) has recently been developed: the hydrolytic condensation of tetraethoxysilane in acetic acid [21]. The main idea underlying this method is that the molecular mass and, hence, the size of silica particles may be controlled via blocking of functional groups at various stages of their growth. In addition, the elaborated synthesis procedures make it possible to change the density of the core, the chemical structure of the organic shell, and the ratio between the inorganic and organic parts of the hybrid particle [22]. These nano-objects are distinguished by their good compatibility with organic solvents, such as THF, toluene, and hexane [23].

The dual nature of molecular silicasols ("macromolecular particles") manifests itself in differently at diverse stages during structure formation. The mechanisms controlling the properties of nanoparticles are provoked not so much by an increase in molecular mass as by intramolecular processes of core densification and the change in the core-to-shell ratio in its structure. At initial stages of formation, the polymer nature is more intrinsic for such objects, while at the final stages, the properties of dense particles both in solution and in the bulk become more typical [24].

Surface modification of particles is a method of attaining chemical similarity between the linear polymer and functional groups at the periphery of functionalized particles. This process should improve their affinity toward the polymer matrix and, in the limit, provide partial mutual solubility of the components.

However, no data are available on the phase equilibrium of mixtures of many pairs of organomodified SiO_2 nanoparticles, although knowledge of phase diagrams makes it possible to reliably select the regions of compositions and temperatures corresponding to their thermodynamic miscibility. At the same time, the specifics of change in rheological properties during the transition from the single-phase region to the two-phase region allows selection of temperature–concentration conditions necessary for successful mixing and processing of such systems in real nanocomposites.

The goal of this study is to investigate the interaction between SiO_2 nanoparticles modified with decyl groups and the polymer close in terms of composition to the grafted groups (polyisobutylene), to construct the phase diagram of such systems, and to examine their rheological properties in wide ranges of composition and temperature.

RESEARCH OBJECTS AND ANALYTICAL PROCEDURES

Nanoparticles were prepared with the use of hyperbranched polyethoxysiloxane that was synthesized as described in [25]. The further modification included two stages.

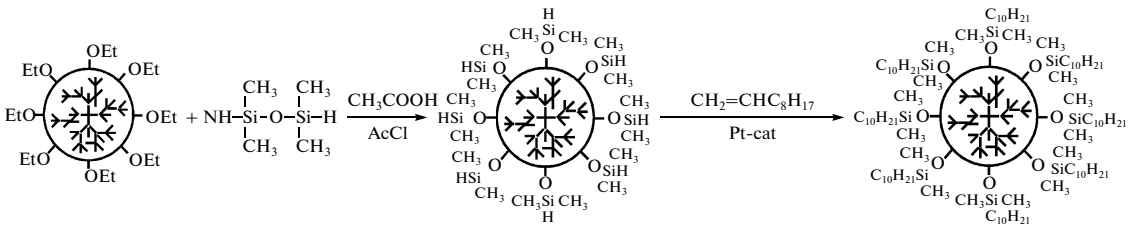

At the first stage, particles with dimethyl hydride silyl surface groups were synthesized. For this purpose, hyperbranched polyethoxysiloxane (50 g, 0.37 mol), tetramethyldisiloxane (100 g, 0.75 mol), acetic acid (350 g, 5.83 mol), and acetyl chloride (0.4 g, 0.005 mol) were mixed. The resulting mixture was boiled for 15–20 h. The condensation reaction was monitored via ^{1}H NMR measurements. The process was conducted until the disappearance of signals at 3.8 ppm due to protons of $-O-CH_2$ ethoxy groups (Fig. 1a). ^{1}H NMR spectra were measured on a Bruker WP-200 SY spectrometer (200.13 MHz); tetramethylsilane was used as an internal standard. The product was washed with toluene to remove acetic acid, and the solvent was removed on a rotor evaporator. The yield of the final product was 71.3 g (98% of the theoretical yield).

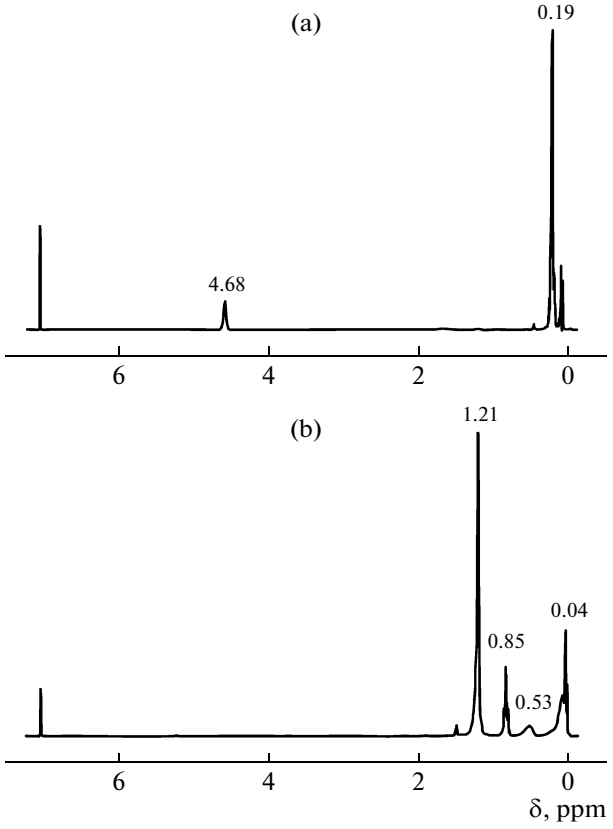

Fig. 1. ^{1}H NMR spectra of (a) nanoparticles with dimethyl hydride silyl surfaces and (b) nanoparticles with decyl end groups.

At the second stage, the product isolated at the first stage of synthesis was hydroxylated. Nanoparticles (6.3 g, 0.0325 mol) with dimethyl hydride silyl surface groups were dissolved in anhydrous toluene (10 mL), Karstedt's catalyst (0.09 mL) was added, and a solution of 1-decene (8 g, 0.057 mol) in anhydrous toluene (17 mL) was loaded. The mixture was heated at 40°C for 15–20 h. The completion of the reaction was checked against the disappearance of ^{1}H NMR signals at 4.7 ppm (Fig. 1b). The reaction mixture was diluted with toluene and passed through a silica gel layer to remove the catalyst. The solvent was distilled off on a rotor evaporator. The yield of the final products was 14.3 g (80% of the theoretical yield). The chromatogram of the nanoparticles with decyl surface groups is shown in Fig. 2a.

Fractionation of modified nanoparticles was performed on a Shimadzu LC-8A liquid preparatory chromatographic system equipped with a Kromasil 300-5SIL column. THF was used as a solvent. Chromatograms of the isolated fractions are shown in Fig. 2b. The solvent was removed first on a rotor evaporator and then evacuated (to 1 mmHg).

Three fractions of nanoparticles (S1, S2, and S3) were used for further studies. The molecular masses and hydrodynamic radii, as estimated from the results of gel-permeation chromatography relative to a polystyrene standard with the use of a universal calibration curve [26], are as follows.

Fraction	S1	S2	S3
Molecular mass	1450	3000	8000
Radius, nm	0.6	0.8	1.1

The as-prepared fractions of nanoparticles are transparent viscous liquids under normal conditions.

The polyisobutylenes (PIBs) Oppanol B10 and Oppanol B11 (BASF) with $M_n = 36 \times 10^3$ and 40×10^3 and polydispersity indexes of 3.0 and 3.2, respectively, were used as complementary linear polymers.

The phase equilibrium of PIB–modified-nanoparticle systems was studied with the use of optical interferometry at 20–200°C via tracing of the evolution of interference bands in the phase-contact zone. The formation of samples and the experiments were per-

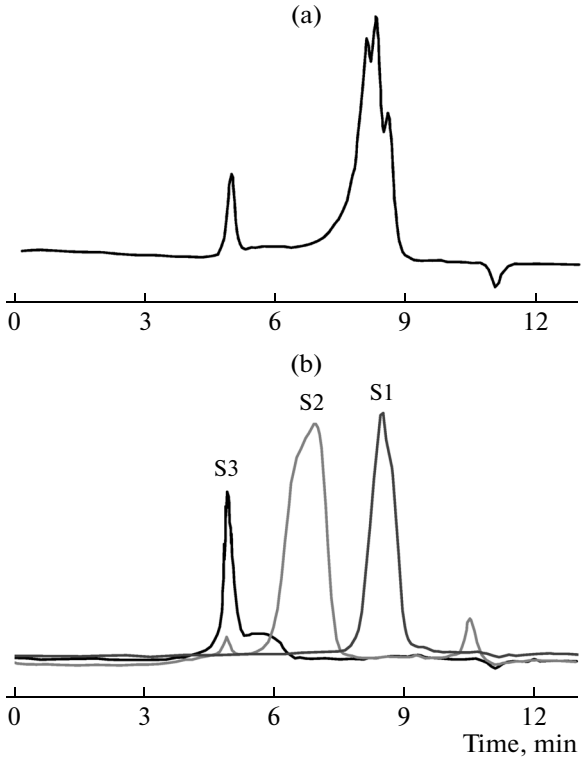

Fig. 2. Chromatograms of (a) initial and (b) fractionated nanoparticles with decyl surface groups.

formed in accordance with the standard procedure [27, 28]. Preassembled cells were held at room temperature for two weeks. The experimental temperature was measured in a stepwise manner; the exposure time at each step was no shorter than 30 min. To confirm the equilibrium state and the reversibility of the measured boundary concentrations, experiments were conducted under regimes of both increasing temperatures and decreasing temperatures.

Rheological characteristics were researched with the use of the following mixtures:

(i) fraction S1 in PIB Oppanol B10 (**S1–B10**) containing 10, 20, 40, 60, 80, 90, and 96 wt % S1;

(ii) fraction S1 in PIB Oppanol B11 (**S1–B11**) containing 34, 43, 56, 66, 74, and 90 wt % S1;

(iii) fraction S2 in PIB Oppanol B10 (**S2–B10**) containing 5, 10, 15, 20, 25, 30, 35, and 44 wt % S2.

Mixing was performed via mechanical stirring at 140°C for several hours. Polymer mixtures with nanoparticles of fraction S3 were not prepared, because of their high viscosities and the impossibility to prepare homogeneous mixture without solvents.

Composite mixtures were studied via rotary rheometry on a Physica MCR 301 (Anton Paar, Austria) device equipped with a cone–plane operating unit (a cone diameter of 8 mm and an angle between the cone generatrix and plane of 1°). Rheological measurements were conducted in two regimes: stationary shear (measurements of flow curves) and oscillatory (dynamic) low-amplitude shear (determination of viscoelastic characteristics).

RESULTS AND DISCUSSION

Phase Equlibrium in Bicomponent Systems

During the contact of nanoparticles with PIB in the diffusion cell, the transition zone reflecting the interdiffusion of components appears spontaneously. For all systems in the transition zone, the phase boundary responsible for amorphous separation of the components is observed (Fig. 3a). An increase in temperature facilitates lengthening of bands near the interface until its disappearance and the formation of a continuous concentration profile (Fig. 3b). Cooling of the solution leads to phase separation accompanied by the formation of droplets of the dispersed phase in the region with an high concentration of nanoparticles (Fig. 3c). The size of the droplets is on the order of 10 μm.

On the basis of boundary concentrations of components in the transition zone that were measured at different temperatures, phase diagrams were constructed (Fig. 4). All systems are characterized by amorphous phase separation with the UCST. Increases in the size of the particles of the modified silica and the molecular mass of PIB are favorable for widening of the two-phase region and a shift of the binodal to high temperatures. For S3-based systems, the right-hand branch of the bimodal merges with the ordinate axis (Fig. 4c). We managed to estimate UCSTs for systems S1–B10 and S1–B11 only; these values were 90 and 135°C, respectively.

Rheology of the Modified Silica

Dependences of viscosity on shear rate for three fractions of the modified silica were obtained through the method of stationary shear flow (Fig. 5a). These objects feature practically Newtonian behavior; that is, their viscosity values are independent of the shear rate. As is known, after functionalization of the surfaces of silica nanoparticles with tertiary ammonium salts, the totality of the solid particles becomes a liquid medium in the absence of any solvent [29]. Moreover, silica nanoparticles with surface-grafted charged functional groups that create an ionic corona around a particle likewise behave as liquids [30]. Hence, the grafting of decyl groups on silica causes a similar transition of the medium from one model of rheological behavior to another.

The absolute value of viscosity increases with an increase in the size of the rigid cores of nanoparticles. In this case, the logarithm of viscosity is proportional to the volume of particles that was calculated in terms of their hydrodynamic radii (Fig. 5b). The slope of the straight line is 0.67, so that, on the basis of this rela-

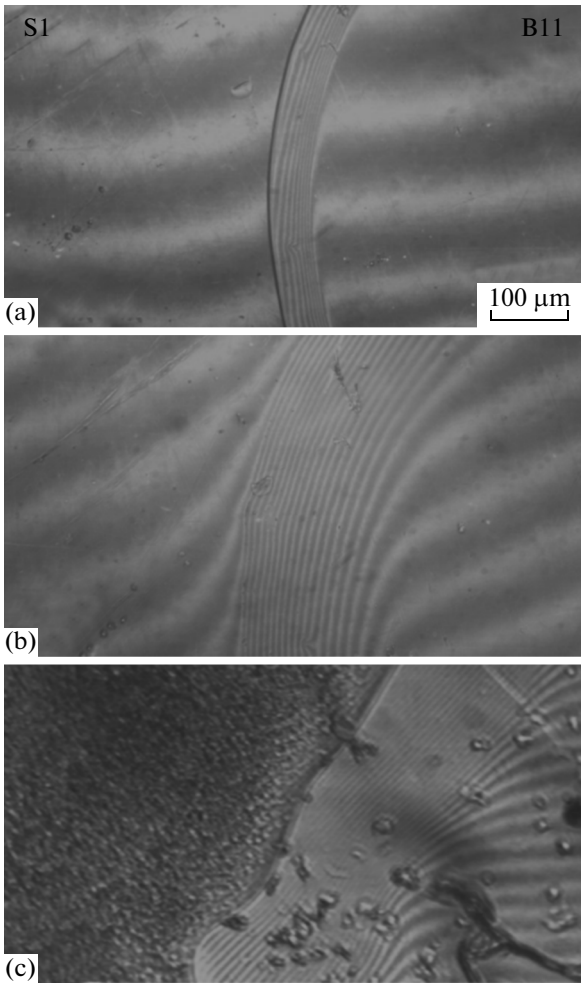

Fig. 3. Interferograms of systems S1–B11 at (a) 40 and (b) 145°C and (c) after further cooling to 25°C.

tionship, the dependence of viscosity of this series of nanoparticles on the size of their cores may be estimated.

Liquid fractions of modified nanoparticles preserve the linear pattern of mechanical behavior until a relative strain on the order of 1% (Fig. 6a) and, in terms of this parameter, take an intermediate position between suspensions of solid particles that form the solidlike structure [31] and polymer solutions or melts [32].

Frequency dependences of the storage modulus and loss modulus when plotted in logarithmic coordinates feature slopes of 1/3 and 1, respectively (Fig. 6b). In accordance with the Maxwell model, the slope of the storage modulus for a simple liquid should be 2.0; a slope of 1/3 is observed for media with the hexagonal morphology [33, 34], for example, for melts of block copolymers with the anisotropic structuring. For nanoparticles with ionic functionalized surfaces, the transition from the model of the simple liquid to the model of the mesophase behavior characterized by a slope of the storage modulus of 1/3 was observed when sulfonate counterions of nanoparticles with silica cores were replaced with isostearate counterions [35].

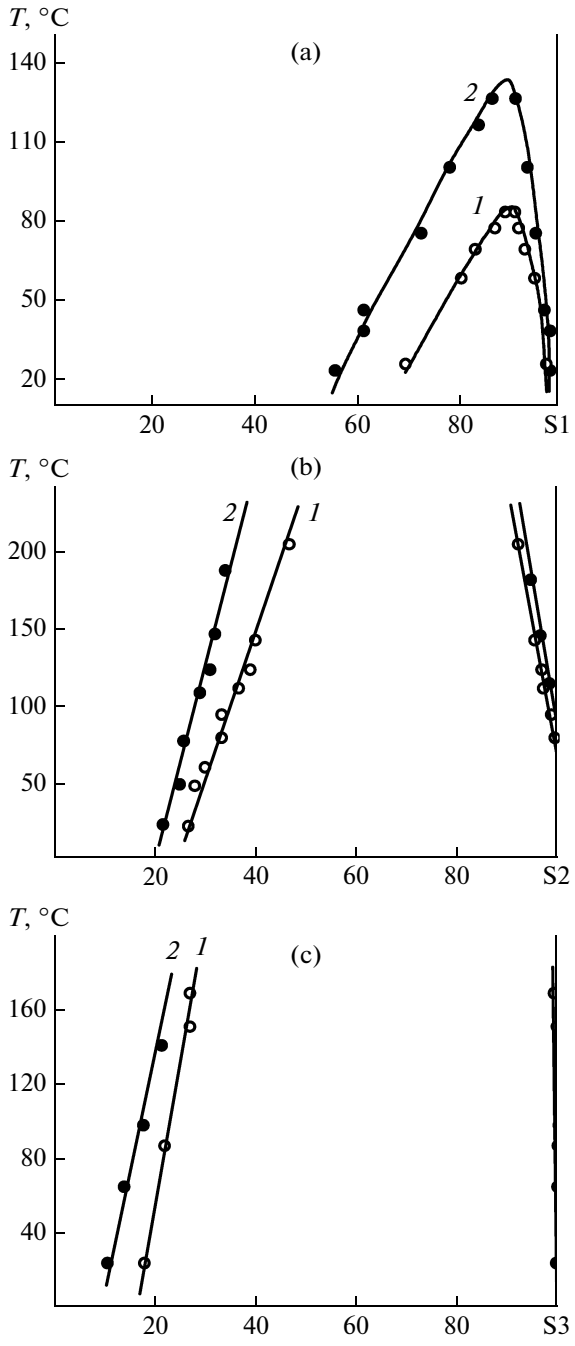

Fig. 4. Phase diagrams of systems (a) S1–PIB, (b) S2–PIB, and (c) S3–PIB: (*1*) sample B10 and (*2*) sample B11.

Rheological Properties of Mixtures in Various Regions of the Phase Diagram

System S1–B10. For S1 mixtures with B10, the dependences of viscosity on shear rate were measured

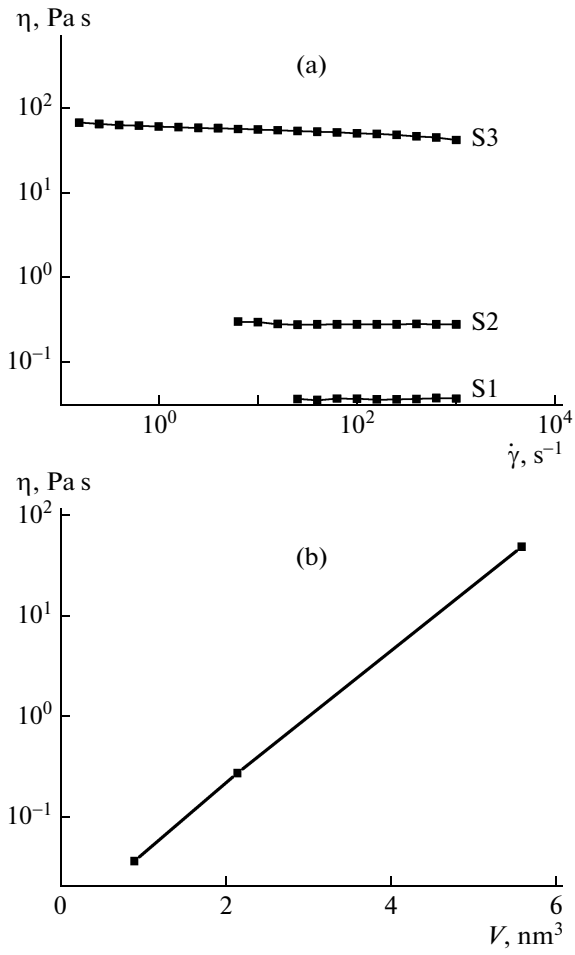

Fig. 5. Plots of viscosity vs. (a) shear rate for fractions S1, S2, and S3 at 20°C and (b) volume of nanoparticles.

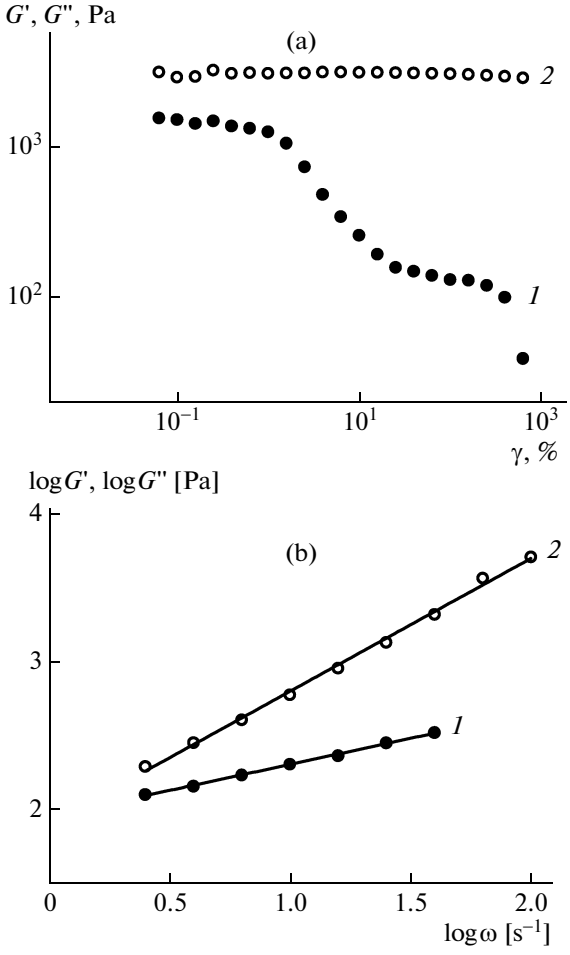

Fig. 6. (a) Amplitude and (b) frequency dependences of (*1*) storage modulus G' and (*2*) loss modulus G'' for sample S3.

at two temperatures, 20 and 90°C (Fig. 7). As is clear from the phase diagram, at 20°C in the range of nanoparticle concentrations from 67 to 97 wt %, this system is heterogeneous and is composed of two phases that are solutions of two compositions, namely, a solution enriched in the polymer (a solution of nanoparticles in the polymer) and a solution depleted of the polymer (a solution of the polymer in a medium of nanoparticles). A temperature of 90°C is close to the critical solution temperature of fraction S1 in the polymer. In accordance with the phase diagram, only beginning from this temperature should the system maintain the homogeneous state throughout the studied concentration range of nanoparticles. Nevertheless, even at lower temperatures, as a result of high viscosity, the system may occur in the metastable state without phase decomposition into solutions with thermodynamically equilibrium concentrations of components owing to kinetic hindrances to mass transfer.

Visual observations show that, at both temperatures for the range of concentrations of nanoparticles in the mixture from 0 to ~60%, the solutions remain transparent and, at least at the optical level, are homogeneous. At high concentrations, the mixtures become turbid and heterogeneous. A change in the phase state of a mixture with an increase in temperature was observed at a concentration of nanoparticles of 80%. If, at 20°C, the mixture of this composition is heterogeneous, then, at 90°C, this mixture is transparent and homogeneous.

All the compositions except the samples containing 60–80% modified nanoparticles are Newtonian liquids. Mixtures for which viscosity increases in a jumpwise manner at a certain shear rate occur near the binodal of the phase diagram (Fig. 4a), where relaxation phenomena are noticeable and where deformation may shift the phase equilibrium to one side or the other. The shear-induced transition has a reversible character, and the system passes into the initial state with a decrease in the rate of mechanical impact (Fig. 8).

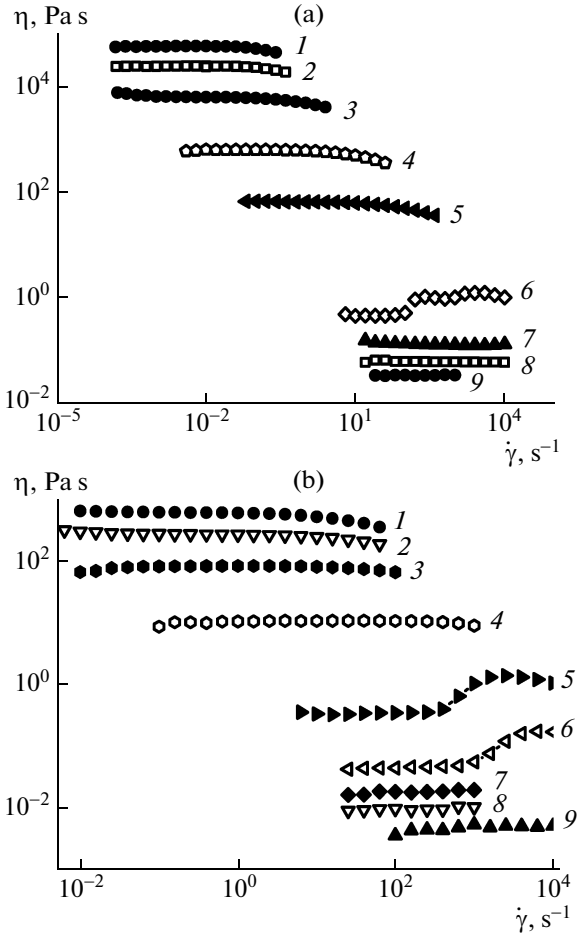

Fig. 7. Plots of viscosity vs. shear rate for mixtures S1–B10 at (a) 20 and (b) 90°C. The contents of S1 in blends are (*1*) 0, (*2*) 10, (*3*) 20, (*4*) 40, (*5*) 60, (6) 80, (*7*) 90, (*8*) 96, and (*9*) 100%.

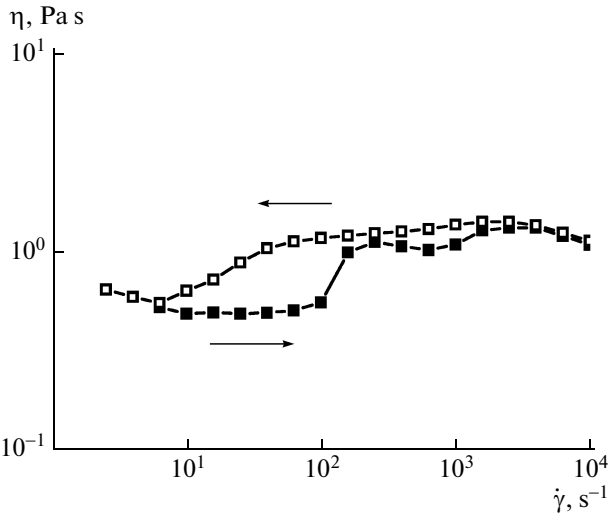

Fig. 8. Evolution of flow curves for an 80% mixture of S1–B10 in cycles of increasing and decreasing shear rate at 20°C. Arrows show the direction of change in the shear rate.

At first glance, the jumpwise gain in viscosity may be associated with a change in composition of the dispersion medium in this sample. In accordance with the phase diagram, at 20°C, the mixture containing 80% fraction S1 is heterogeneous and the ratio between the amount of the "solution of nanoparticles in the polymer" phase and the amount of the "solution of the polymer in the medium of nanoparticles" system is 1 : 1.4. It is assumed that, at low shear rates ($\dot{\gamma} < 100$ s^{-1}), the latter phase as a phase depleted of the polymer and having a lower viscosity functions as the dispersion medium. In contrast, at high shear rates, the first phase, that is, the solution enriched with the polymer, becomes the dispersion medium.

However, the above suggestion is disproved by tests performed at 90°C. As was mentioned above, at 90°C, the compositions should be homogeneous. Nevertheless, as is seen from dependences of viscosity on shear rate (Fig. 5b), the viscosity of the samples likewise increases in a jumpwise manner. Note that this effect manifests itself at a lower content of nanoparticles (60%) and is preserved as their concentration is increased to 80%. At a content of nanoparticles of 60%, an increase in viscosity occurs at a shear rate of $\dot{\gamma} > 250$ s^{-1}; at a content of nanoparticles of 80%, an increase in viscosity occurs at a shear rate of $\dot{\gamma} > 650$ s^{-1}.

In general, the results of rheological and interferometry measurements should be compared with caution. The nanoparticles have highly developed specific surfaces; that is, their behavior is markedly affected by their surface properties, which substantially differ from the bulk properties of common materials with nonmodified surfaces. When studying compatibility, an experimenter primarily estimates the interaction of a solvent with the surfaces of nanoparticles, whereas flow curves of the composite are determined by the hydrodynamic effects of nanoparticles as a whole, that is, by their bulk properties.

Deformation may shift the lines of phase equilibrium to both the side of homogenization and the side of "heterogenization" [36–39]. At 20°C, under equilibrium conditions, the system containing 80% S1 occurs in the region of insolubility of the components. Shear stress appearing during viscosity measurements apparently entails a mechanical-field-induced transition to the homogeneous region, as reflected by a gain in viscosity at shear rates above 100 s^{-1} (Fig. 8). As the shear rate is decreased, the reversible transition to the region of immiscibility of the components occurs.

The concentration dependences of viscosity for homogeneous and heterogeneous systems are described by different dependences (Fig. 9), but in both cases, they are linear when plotted in semilogarithmic coordinates. Because the positions of the lines

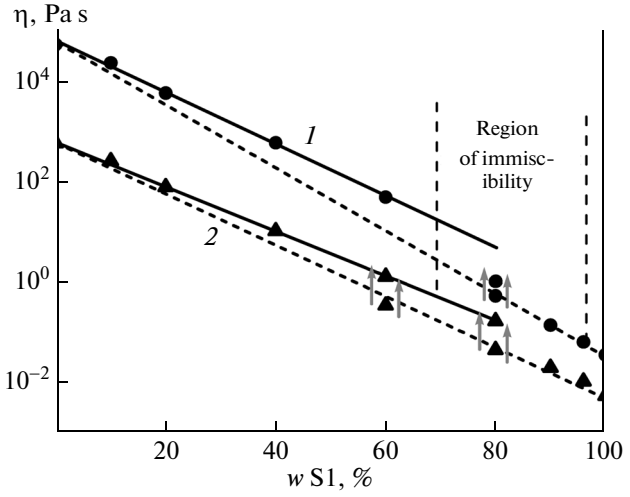

Fig. 9. Concentration dependences of viscosity for system S1–B10 at (*1*) 20 and (*2*) 90°C. Arrows show the shear-induced transition, and dashed lines represent the additivity dependences.

of phase equilibrium change under shear, the jumpwise transition from one dependence to another is observed (shown by arrows in Fig. 9) during viscosity measurements with an increase in shear rate.

The viscosity of the binary polymer mixture, $\eta_{1,2}$, under the condition that the contributions of components obey the additivity rule (the absence of specific interactions between components), is described by the logarithmic additivity of the viscosities of the components:

$$\ln \eta_{1,2} = c_1 \ln \eta_1 + c_2 \ln \eta_2 \quad (1)$$

Here, c_1 and c_2 are the concentrations of the individual components with viscosities η_1 and η_2, respectively. Equation (1) is applicable for ideal liquid mixtures, in which intermolecular interactions are identical for similar and dissimilar molecules, and should be applicable in the first approximation for the complementary polymer and the surfaces of nanoparticles.

Experimental data for samples with high contents of fraction S1 (above 80%) are well described by the additive curve, whereas for the concentration range of nanoparticles from 10 to 80%, deviation of the samples from the additivity law increases with the filler fraction. This situation is probably associated with the difference in the energies of interaction between the polymer and nanoparticles in their solution and the energies of interaction typical for individual compounds. Because the strength of bonding between nonpolar polymer and nonpolar surfaces of nanoparticles should not depend on their ratio in the mixture, the solution of components is specific to the entropy factor. Nanoparticles show much better solubility in the polymer but not vice versa; therefore, the gain in entropy related to the distribution of nanoparticles in the polymer is higher than the gain in entropy related to an increase in the flexibility of polymer chains. Limited solubility indicates a positive value of enthalpy during dissolution. In turn, a negative value of the heat of transition should lead to a negative change in its temperature upon loading [39]. This is in fact the case: During shear of the samples, the transition of their viscosities from values typical for the additivity (mixture) dependence to the dependence typical for homogeneous solutions occurs.

In general, deformation of the mixture samples should cause orientation and a decrease in the entropy of polymer chains; as a result, miscibility should worsen. Moreover, shear facilitates an increase in entropy owing to mixing of the components and dispersing of nanoparticles. In [40], the stable volume of particles of the new phase in an intense mechanical field was estimated through the relationship

$$V = (0.74\varsigma / \eta\dot{\gamma})^3, \quad (2)$$

where ς is the interfacial tension and η is the viscosity of the dispersion medium.

The estimation of surface tension via the pendant-drop method yielded $\varsigma = 23.3$ mN/m for fraction S1 and $\varsigma = 31.8$ mN/m for the polymer [41], and the measured contact angle for the droplet of nanoparticles on the surface of PIB was 7°. Thus, the interfacial tension at the boundary of system S1–B10 was calculated as 9.1 mN/m.

Then, on the basis of Fig. 7 (the viscosity and the maximum shear rate not causing the jumpwise transition) and Eq. (2), the diameters of stable particles of the dispersed phase may be calculated. For the system containing 80% fraction S1 at 20°C, the diameter of stable droplets of the polymer (or, in accordance with the phase diagram, a concentrated solution of the polymer) is 50 μm. Dissolution of the polymer during an increase in shear rate causes a marked gain in viscosity of the dispersion medium and leads to a reduction in the calculated diameter of stable objects to 0.7 μm. The same calculation for this system at 90°C indicates that the diameters of particles of the dispersion phase before and after the shear-induced phase transition are 5.6 and 0.16 μm, respectively. The latter value corresponds to the condition of optical transparency and indirectly confirms the presence of nanometer, but not elementary, structures in homogeneous, in accordance with the interferometry studies, samples. In other words, the transition from microphase structures to nanophase structures of the samples occurs during dissolution; as a consequence, their optical and rheological properties change sharply.

It should be mentioned that, in accordance with the phase diagram, the mixture containing a small amount of the polymer at 90°C should be homogeneous. However, as evidenced by rheological testing and visual observations, this is not true. This discrepancy has been explained above by transition phenom-

ena near the binodal and the difference in bulk and surface properties. In addition, it is reasonable to discuss another cause related to the "colloidal" behavior of practically spherical nanoparticles in the polymer matrix. Here, it may be a good thing to draw an analogy with surfactants that, at concentrations above the critical concentration, form micellar structures that in some cases are responsible for the well-defined non-Newtonian behavior of a solution [42–44]. Functionalized nanoparticles are similar to spherical micelles in terms of structure and shape; moreover, it is not inconceivable that, if there are nonmodified defect regions on their surfaces, particles show a tendency toward aggregation accompanied by the formation of extended aggregates or even chains.

Hence, even in the region of single-phase solutions near the bimodal, equilibrium or nonequilibrium ordered aggregates may exist; their presence is registered via rheological methods.

During viscosity measurements at various temperatures, the transition from the homogeneous system to the heterogeneous system was observed as well. The temperature dependence of viscosity obtained for the sample containing 80% fraction S1 shows a step corresponding to the phase transition, as evidenced by the phase diagram of this system (Fig. 10). The jumpwise decrease in viscosity occurs in the range 36–50°C, that is, at temperatures below those expected in accordance with the phase diagram, in consistency with an increase in the solubility of nanoparticles observed for the polymer during application of a mechanical field.

On the basis of the temperature dependence of viscosity plotted in Arrhenius coordinates, the activation energy of viscous flow may be calculated, that is, the excess energy assumed by the kinetic units of the system that is sufficient for hopping from one position to another. It was found that the activation energies of flow for homogeneous and heterogeneous mixtures differ by a factor of almost 2 (Fig. 11); do not depend on the ratio of components in the mixture; and, in the limit, coincide with the activation energies of modified nanoparticles (for heterogeneous samples) and the polymer (for homogeneous samples).

To gain insight into the effect of small amounts of nanoparticles on the relaxation properties of systems S1–B10, the dynamic testing of samples of various compositions was performed (Fig. 12a). Nanoparticles in the mixture play the role of a plasticizing agent and decrease the storage modulus and loss modulus. The slope of the tangent of the initial portion of the frequency dependence of the loss modulus equal to 1.0 is preserved during dilution, while the storage modulus decreases to 1.6, thereby evidencing an increase in the polydispersity of the sample. The quantitative characteristics of relaxation properties may be estimated

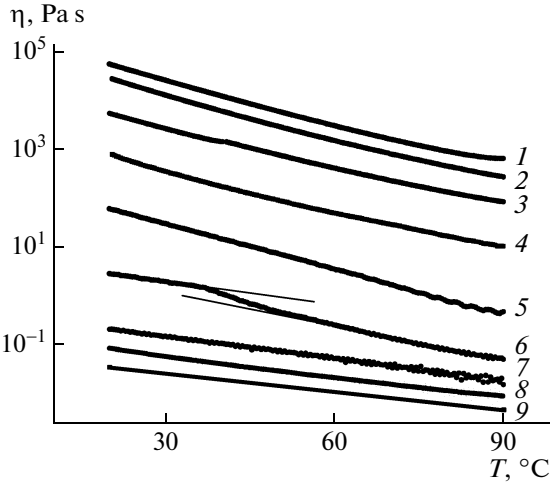

Fig. 10. Temperature dependences of viscosity for systems S1–B10 measured during cooling of the samples at a rate of 5 K/min. The concentrations of S1 in mixtures are (*1*) 0, (*2*) 10, (*3*) 20, (*4*) 40, (*5*) 60, (*6*) 80, (*7*) 90, (*8*) 96, and (*9*) 100%.

through calculation of the continuous relaxation spectrum of the system under the assumption that it may be described by the following formula [45]:

$$G(\tau) = K_0\tau^{-\alpha}, \quad (3)$$

where G is the fraction of relaxation time τ in the relaxation spectrum, K_0 is the intensity of this relaxation time, α is the slope of the spectrum characterizing polydispersity over time, and τ is the maximum relaxation time.

It was found that an increase in the content of nanoparticles is accompanied by linear decreases in the logarithms of the maximum relaxation time and pre-exponential factor K_0, which characterizes the rubberlike elasticity of the system. This finding reflects the plasticization effect of the high-molecular-mass object with the low-molecular-mass object with an increase in the volume faction of the latter compound. Exponent α characterizes the slope of the rubberlike-elasticity plateau, and its linear increase is associated with the gain in the polydispersity of the system due to the presence of dissolved nanoparticles (Fig. 12b).

System S1–B11. The rheological behavior of mixtures S1–B11 characterized by higher molecular masses of the polymer is qualitatively similar to the above dependence (Fig. 13). An analysis of the dependences of viscosity on shear rate showed that homogeneous, as follows from the phase diagram (Fig. 4), samples are Newtonian liquids. Heterogeneous mixtures can undergo homogenization during shear, as reflected by the dilatant behavior, that is, an increase in viscosity with the shear rate. Dissolution during shear is well seen in the case of curves measured at 20°C and corresponding to amounts of modified nanoparticles of 66 and 74%. In this case, shear rates

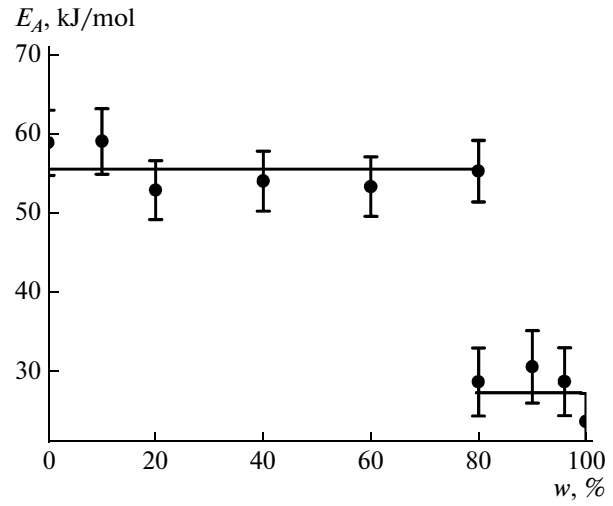

Fig. 11. Concentration dependence of the activation energy of viscous flow of system S1–B10.

leading to a gain in viscosity of this system coincide with shear rates that exert the same effect in the case of system S1–B10. In the samples tested at a temperature above the UCST, there are no shear-induced transitions.

As in the previous case, the improvement of solubility during shearing is probably related to the entropy factor owing to dispersion of the components in each other. In other words, the phenomenon is of the kinetic character and is not associated with a change in the temperature of the phase transition [39].

The concentration dependences of viscosity are linearized in semilogarithmic coordinates for both homogeneous and heterogeneous systems (Fig. 14). The extrapolation of straight lines describing the behavior of homogeneous and heterogeneous systems to the zero concentration of the polymer leads to the same value, equal to the viscosity of the modified nanoparticles. This circumstance is illustrated by the fact that homogeneous samples are characterized by an increase in viscosity related to the presence of the high-molecular-mass component dissolved in the system of modified nanoparticles. Because of a higher molecular mass of the polymer, the heterophase state of the system is observed at a smaller content of nanoparticles than that in the case of the previous system. Thus, an increase in the molecular mass of the polymer worsens the miscibility of the components, in agreement with the interferometry data.

System S2–B10. The dependences of viscosity on shear rate for systems S2–B10 differ qualitatively from the above dependences (Fig. 15). Depending on composition, the curves and the objects described by these curves may be divided into two groups. The flow of the first group is similar to the flow of the unfilled polymer; that is, there is an extended branch of the zero-shear viscosity up to high shear rates followed by the transition to the spurt regime (the induced rubbery elasticity regime). This behavior is preserved up to a concentration of nanoparticles of 20% and is inherent to the region of full solubility of the components (Fig. 4b).

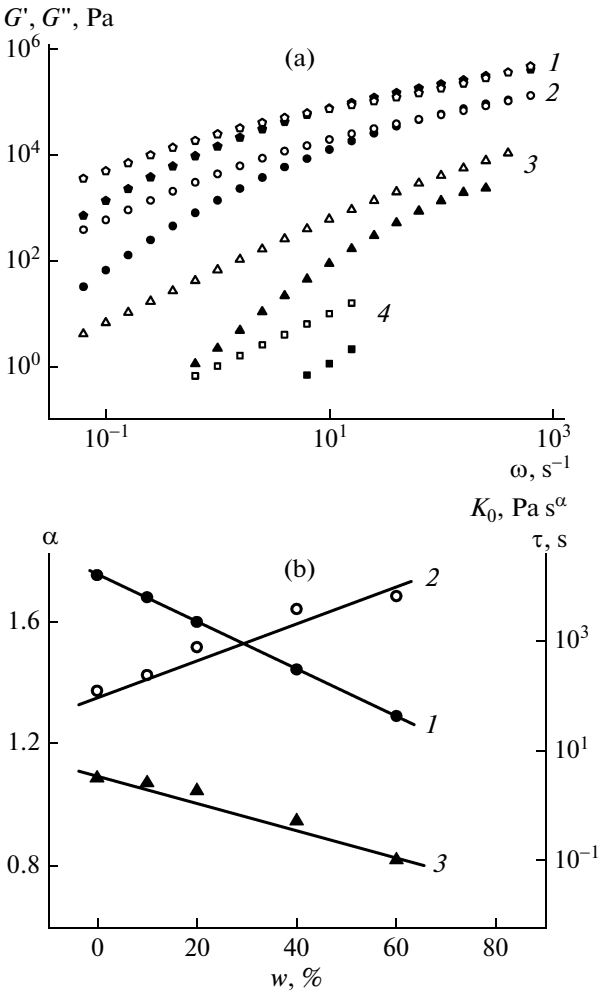

Fig. 12. (a) Frequency dependences of the components of the complex dynamic modulus at 20°C for system S1–B10 and (b) dependences of the characteristics of the continuous relaxation spectrum on the content of nanoparticles in system S1–B10. (a) Closed circles refer to G', and open circles refer to G''; the concentrations of S1 are (*1*) 0, (*2*) 20, (*3*) 60, and (*4*) 80%; (b) (*1*) K_0, (*2*) α, and (*3*) τ.

The second group of objects with a higher concentration of modified nanoparticles is characterized by a narrow region of Newtonian flow and a sharp decline in viscosity with an increase in shear rate.

The non-Newtonian pattern of flow at 20°C indicates the heterogeneous state of the systems in accordance with the phase diagram and may reflect the destruction of contacts between particles (droplets) of the dispersed phase and their orientation in

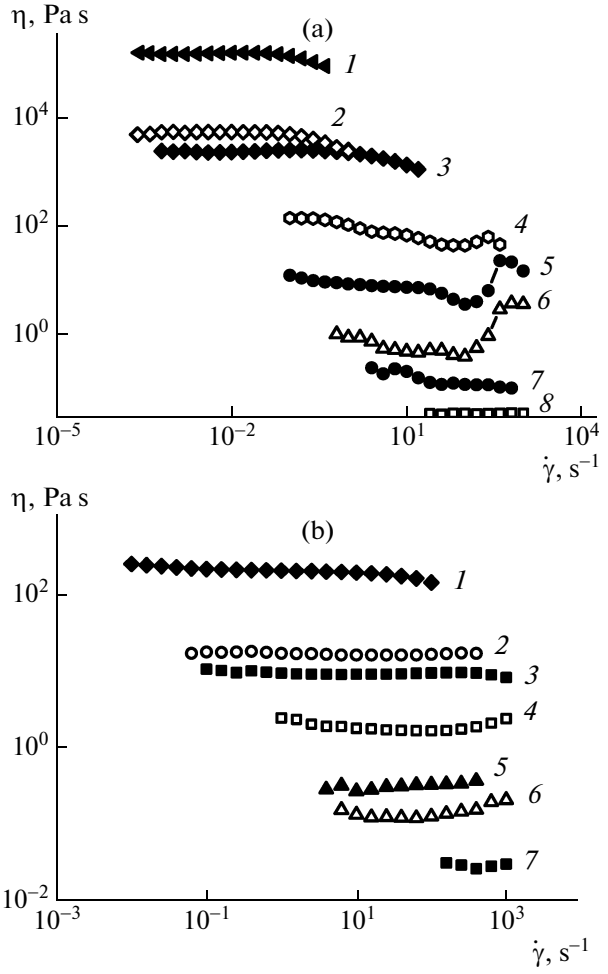

Fig. 13. Plots of viscosity vs. shear rate for mixtures S1–B11 at (a) 20 and (b) 140°C. The concentrations of nanoparticles in the mixture are (*1*) 0, (*2*) 34, (*3*) 43, (*4*) 56, (*5*) 66, (*6*) 74, (*7*) 90, and (*8*) 100%.

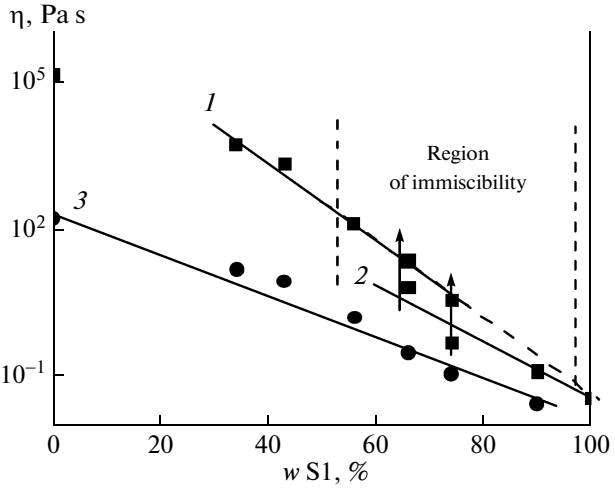

Fig. 14. Concentration dependences of viscosity for system S1–B11 at (*1*, *2*) 20 and (*3*) 140°C: (*1*, *3*) for homogeneous systems and (*2*) for heterogeneous systems.

flow. Because the viscosities of heterogeneous systems are smaller than the viscosities of homogeneous systems, nanoparticles play the role of the dispersion medium, while the polymer functions as the dispersed phase throughout the region of heterophase compositions.

At 110°C, the non-Newtonian character becomes more pronounced. Note that the patterns of concentration dependences of viscosity for homogeneous and heterogeneous systems are different (Fig. 16). This is evident from the different slopes of linear dependences obtained at 20°C in semilogarithmic coordinates. In addition, in accordance with the phase diagram, at 110°C, the systems containing less than 30% nanoparticles are likewise homogeneous, as evidenced by the fact that the slope is equal to that for homogeneous (at 20°C) systems. Thus, the non-Newtonian behavior observed at 110°C is apparently related to the phase decomposition of the solution under the effect of shear.

With respect to the above experiments, an increase in the size of nanoparticles and, accordingly, a reduction in their total amount in the system lead to the situation where the entropy gain due to the dispersive effect of shear stress is not so high, whereas the entropy decrease related to the orientation of PIB chains in flow is maintained at the same level. Thus, when the nanoparticles are small, they control the behavior of the mixture; when the nanoparticles are larger, the polymer assumes the decisive role.

The phase transition during shearing is reversible, as evidenced by the thixotropic behavior of the sample: a change in the position of the flow curve with a decrease in the shear rate (Fig. 17). The rate of shear at which decomposition occurs depends on temperature. For example, for the system containing 35% nanoparticles, phase separation at 140°C is observed at a shear rate that is a factor of 6 greater than that at 110°C. This finding reflects the fact that an increase in temperature entails the improvement of affinity between the components (the system with the UCST).

Thus, an increase in the molecular mass of nanoparticles, that is, an increase in the volume fraction of the rigid core, leads to the transition to the two-phase region under the action of shear, rather than to homogenization of the system. This is the key difference in the role of shear in phase transitions of the systems based on fractions S1 and S2. Figure 18 schematically shows the shift of binodal curves during shear for filled samples with nanoparticle diameters smaller or larger than a certain critical value. Note that, on the basis of the above data, the effects of shear on the position of the UCST and, accordingly, on the direction (concentration or temperature) of the phase-diagram shifts cannot be estimated. In addition, for systems with very small particles, the shift in the transition temperature is

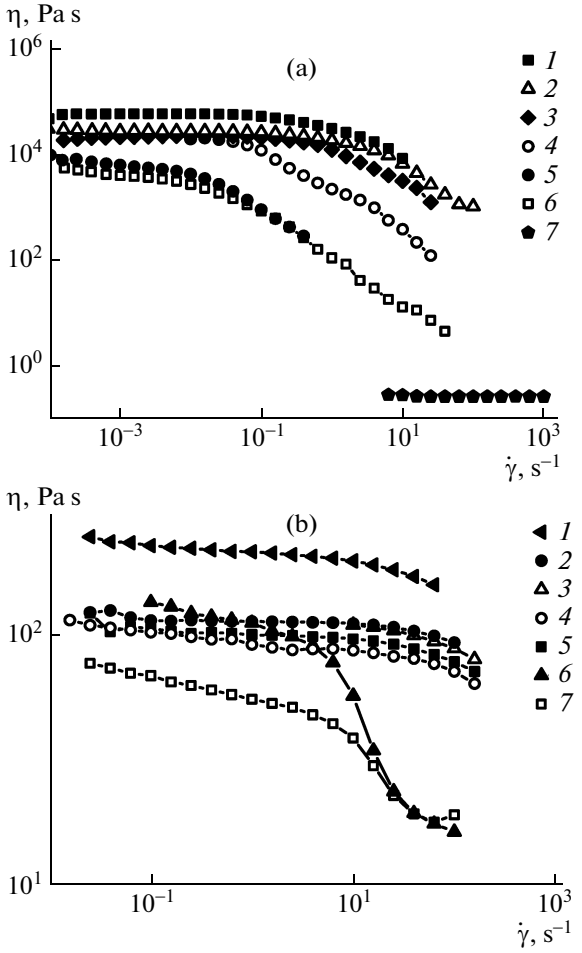

Fig. 15. Plots of viscosity vs. shear rate for mixtures S2–B10 at (a) 20 and (b) 110°C. The concentrations of nanoparticles are (a) (*1*) 0, (*2*) 5, (*3*) 20, (*4*) 25, (*5*) 35, (*6*) 44, and (*7*) 100% and (b) (*1*) 0, (*2*) 5, (*3*) 10, (*4*) 15, (*5*) 20, (*6*) 25, and (*7*) 35%.

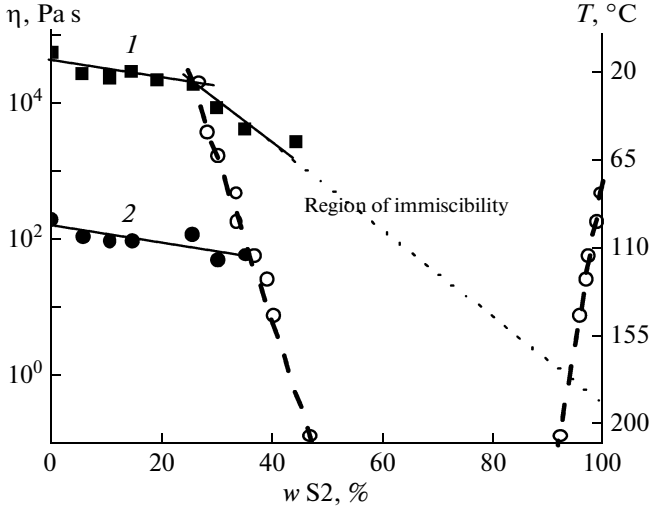

Fig. 16. Concentration dependences of viscosity at zero shear for system S2–B10 at (*1*) 20 and (*2*) 110°C. The phase diagram is shown by the dotted line.

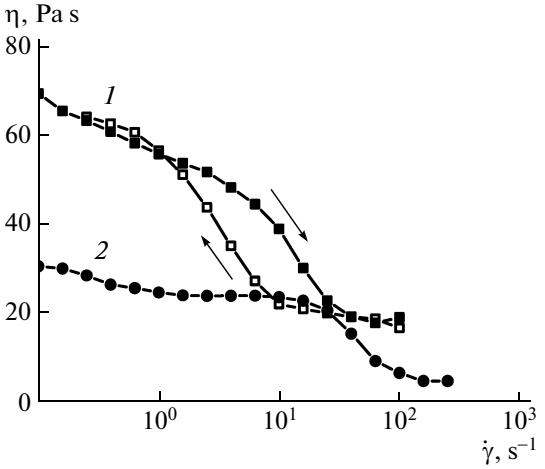

Fig. 17. Flow curves for a 35% mixture of S2–B10 at (*1*) 110 and (*2*) 140°C. For 110°C, the evolution of the dependence is shown in cycles of increasing and decreasing shear rate.

related to the kinetic factor due to the forced mixing of the components, whereas, in the case of samples with larger nanoparticles, the temperature of phase separation apparently shifts because of changes in the thermodynamic characteristics of macromolecules.

CONCLUSIONS

Functionalization of the surfaces of silica nanoparticles causes a unusual effect: Nanoparticles in the bulk are a liquid viscoelastic medium with Newtonian flow. Note that their behavior is in conflict with the Maxwell model developed for simple liquids, but is qualitatively similar to the behavior of anisotropic systems with the cylindrical morphology. The viscoelastic characteristics of such systems increase exponentially with the sizes of the inorganic cores, which constitute slice of a nanometer.

The presence of nonpolar organic groups on the surfaces of particles makes them miscible with the complementary polymer; the smaller the cores of the nanoparticles and the molecular mass of the polymer, the better the solubility. The miscibility of two components improves with temperature, and their phase behavior is described by the diagram with the UCST. However, the presence of the rigid inorganic cores in nanoparticles with surfaces modified with organic groups gives no way of drawing an analogy between miscibility and mutual dissolution. Most probably, the case in point is the micro- or nanophase uniform distribution of nanoparticles in the matrix of the linear polymer and vice versa. It is important that solubility

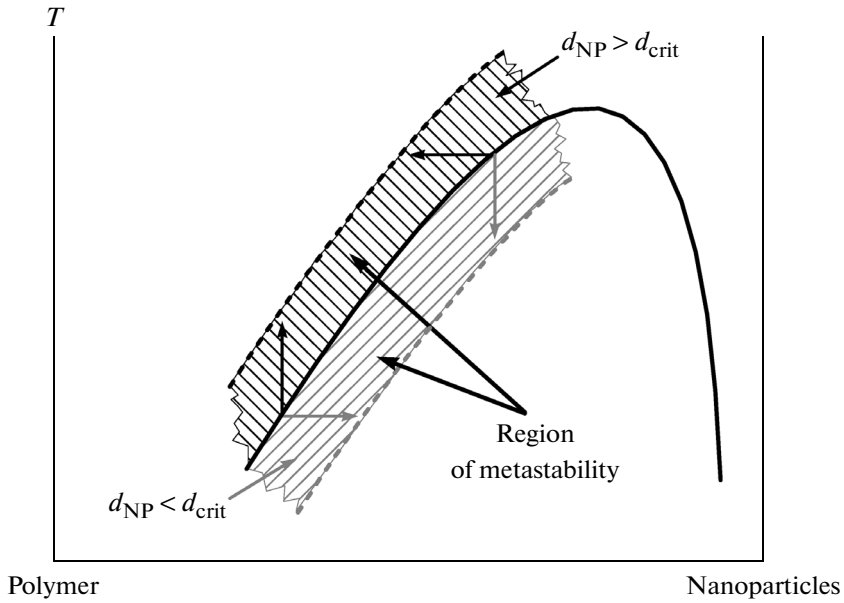

Fig. 18. Evolution of the phase diagram under the effect of shear on the nanocomposites with larger or smaller sizes of nanoparticles (NPs).

depends on the external mechanical effect and, under shear, improves in the case of small particles and worsens in the case of large particles. For miscible components, less viscous nanoparticles plasticize the polymer; in the region of immiscibility, heterogeneous systems are emulsions.

The rheological characteristics of the complex solution depend on the concentration of modified nanoparticles and the sizes of their inorganic cores, a circumstance that opens new possibilities for their targeted variation.

ACKNOWLEDGMENTS

We are grateful to A.M. Muzafarov and O.A. Serenko (Enikolopov Institute of Synthetic Polymer Materials, Russian Academy of Sciences) for valuable discussion of the results of this study.

This work was supported by the Russian Foundation for Basic Research, project no. 14-03-31810 mol_a.

REFERENCES

1. M. Xanthos, *Functional Fillers for Plastics* (Wiley-VCH Verlag, Berlin, 2010).
2. F. Gao, *Advances in Polymer Nanocomposites* (Woodhead Publ., Cambridge, 2012).
3. L. Nicolais and G. Carotenuto, *Metal-Polymer Nanocomposites* (Wiley, Hoboken, 2005).
4. V. Favier, H. Chanzy, and J. Y. Cavaille, Macromolecules **28** (18), 6365 (1995).
5. Y. Zhou, S. Yu, C. Wang, et al., Chem. Commun. **13**, 1229 (1999).
6. R. A. Vaia, B. B. Sauer, O. K. Tse, and E. P. Giannelis, J. Polym. Sci., Polym. Phys. Ed. **35** (1), 59 (1997).
7. M. Moniruzzaman and K. I. Winey, Macromolecules **39** (16), 5194 (2006).
8. M. S. Wang and T. J. Pinnavaia, Chem. Mater. **6** (4), 468 (1994).
9. P. Podsiadlo, A. K. Kaushik, E. M. Arruda, et al., Science **318** (5847), 80 (2007).
10. E. P. Giannelis, Appl. Organomet. Chem. **12**, 675 (1998).
11. T. Kashiwagi, F. Du, J. F. Douglas, et al., Nature Mater. **4**, 928 (2005).
12. R. Gangopadhyay and A. De, Chem. Mater. **12** (3), 608 (2000).
13. R. A. Vaia, S. Vasudevan, W. Krawiec, et al., Adv. Mater. **7** (2), 154 (1995).
14. H. Zou, S. Wu, and J. Shen, Chem. Rev. **108** (9), 3893 (2008).
15. M. Tanahashi, Materials **3** (3), 1593 (2010).
16. O. Aso, J. I. Eguiazarbal, and J. Nazarbal, Compos. Sci. Technol **67**, 2854 (2007).
17. H. Sertchook, H. Elimelech, C. Makarov, et al., J. Am. Chem. Soc. **129**, 98 (2007).
18. M. Z. Rong, M. Q. Zhang, and W. H. Ruan, Mater. Sci. Technol **22** (7), 787 (2006).
19. S.-W. Zhang, S.-X. Zhou, Y.-M. Weng, and L.-M. Wu, Langmuir **21**, 2124 (2005).
20. M. Nakamura, US Patent No. 0330582 (2010).
21. V. V. Kazakova, A. S. Zhiltsov, O. B. Gorbatsevitch, et al., J. Inorg. Organomet. Polym. Mater **22** (3), 564 (2012).
22. L. A. Novokshonova, P. N. Brevnov, V. G. Grinev, et al., Nanotechnol. Russ. **3** (5–6), 330 (2008).

23. N. V. Voronina, I. B. Meshkov, V. D. Myakushev, et al., Nanotechnol. Russ. **3** (5–6), 321 (2008).
24. N. V. Voronina, I. B. Meshkov, V. D. Myakushev, et al., J. Polym. Sci., Part A: Polym. Chem. **48**, 4310 (2010).
25. V. V. Kazakova, E. A. Rebrov, V. D. Myakushev, et al. in *Am. Chem. Soc. Symp. Book Series 729*, Ed. by S. J. Clarson, J. J. Fitzgerald, M. J. Owen, and S. D. Smith (Am. Chem. Soc, New York, 2000).
26. Z. Grubisic, R. Rempp, and H. Benoir, J. Polym. Sci., Part B: Polym. Phys. **5**, 753 (1967).
27. A. E. Chalykh, V. K. Gerasimov, and Yu. M. Mikhailov, *Phase State Diagrams of Polymer Systems* (Yanus-K, Moscow, 1998) [in Russian].
28. V. Makarova and V. Kulichikhin, *Interferometry. Research and Applications in Science and Technology*, Ed. by I. Padron (InTech, Rijeka, 2012).
29. A. B. Bourlinos, R. Herrera, N. Chalkias, et al., Adv. Mater. **17**, 234 (2005).
30. R. Rodriguez, R. Herrera, L. A. Archer, and E. P. Giannelis, Adv. Mater. **20**, 4353 (2008).
31. S. Ilyin, V. Kulichikhin, and A. Malkin, Appl. Rheol **24** (1), 13653 (2014).
32. S. O. Ilyin, A. Ya. Malkin, and V. G. Kulichikhin, Polym. Sci., Ser. A **56** (1), 98 (2014).
33. M. B. Kossuth, D. C. Morse, and F. S. Bates, J. Rheol **43**, 167 (1999).
34. C. Y. Ryu, M. S. Lee, D. A. Hajduk, and T. P. Lodge, J. Polym. Sci., Part B: Polym. Phys. **35**, 2811 (1997).
35. A. B. Bourlinos, E. P. Giannelis, Q. Zhang, et al., Eur. Phys. J. **20**, 109 (2006).
36. A. E. Chalykh and V. K. Gerasimov, Russ. Chem. Rev. **73** (1), 59 (2004).
37. S. A. Vshivkov and E. V. Rusinova, Polym. Sci., Ser. A **36** (1), 81 (1994).
38. S. V. Kotomin, S. O. Il'in, T. N. Filippova, and G. K. Shambilova, Polym. Sci., Ser. A **55** (3), 186 (2013).
39. A. Ya. Malkin and S. G. Kulichikhin, Polym. Sci., Ser. B **38** (2), 362 (1996).
40. W. Kuhn, H. Majer, and F. Burkhardt, Helv. Chim. Acta **43** (5), 1208 (1960).
41. H. Edwards, J. Appl. Polym. Sci. **12** (10), 2213 (1968).
42. T. M. Clausen, P. K. Vinson, J. R. Minter, et al., J. Phys. Chem. **96** (1), 474 (1992).
43. E. K. Wheeler, P. Izu, and G. G. Fuller, Rheol. Acta. **35** (2), 139 (1996).
44. L. M. Walker, Curr. Opin. Colloid Interface Sci **6**, 451 (2001).
45. A. Ya. Malkin, Polym. Sci., Ser. A **48** (1), 39 (2006).

Trnaslated by T. Soboleva